Weak Temperature Dependence of Ageing of Structural Properties in Atomistic Model Glassformers

Thomas Jenkinson,[1] Peter Crowther,[1] Francesco Turci,[1] and C. Patrick Royall[1, 2, 3, 4]
[1)] *H.H. Wills Physics Laboratory, Tyndall Avenue, Bristol, UK*
[2)] *School of Chemistry, University of Bristol, Cantock's Close, Bristol, UK*
[3)] *Centre for Nanoscience and Quantum Information, Tyndall Avenue, Bristol, UK*
[4)] *Department of Chemical Engineering, Kyoto University, Kyoto 615-8510, Japan*[a)]

Ageing phenomena are investigated from a structural perspective in two binary Lennard-Jones glassformers, the Kob-Andersen and Wahnström mixtures. In both, the geometric motif assumed by the glassformer upon supercooling, the locally favoured structure (LFS), has been established. The Kob-Andersen mixture forms bicapped square antiprisms, the Wahnström model forms icosahedra. Upon ageing, we find that the structural relaxation time has a time-dependence consistent with a power law. However the LFS population and potential energy increase and decrease respectively, in a logarithmic fashion. Remarkably, over the timescales investigated, which correspond to a factor of 10^4 change in relaxation times, the *rate* at which these quantities age appears almost independent of temperature. Only at temperatures far below the Vogel-Fulcher-Tamman temperature do the ageing dynamics slow.

I. INTRODUCTION

Though glasses have been widely used for millennia, the underlying process through which they form is not well understood and the glass transition remains one of the "largest unanswered questions in solid state physics"[1]. Glasses are materials which are characterised by two key properties. Firstly, they show structural disorder in the arrangement of the constituent atoms or molecules. Secondly, they have such extremely slow dynamical behaviour that their the relaxation is not measurable on experimental timescales. This second characteristic means that glasses are by their nature out of equilibrium. As glasses move towards equilibrium, their physical properties such as relaxation time and the average energy per particle evolve over time, a phenomenon which is termed ageing[2,3].

We express ageing by the waiting time, t_w, which is the time between the perturbation of the system from equilibrium and the time at which the properties of the system are measured. The dynamics of ageing systems have been the topic of considerable scrutiny[4–15], among the most striking observations being that relaxation time increases as a function of waiting time[16]. Recent work by Gujrati[17] places the earlier phenomenological Tool—Narayanaswamy[18,19] approach on a somewhat firmer footing: the "fictive temperature" follows a logarithmic relationship, although at small waiting times, some systems exhibit an exponential increase in the relaxation time. Other work finds a power law behaviour in the waiting time, although the rate of increase in relaxation time is reduced on timescales comparable to the waiting time[10]. This is particularly relevant since it concerns one of the binary Lennard-Jones models considered in this work.

Historically, the lack of structural difference between a liquid and a solid glass was considered one of the most mysterious properties of glasses[2,16]. In part, this is a consequence of considering only two-point structural correlation functions such as the pair correlation function $g(r)$ where structural changes are very small but not completely absent[20]. In recent years, a consensus has emerged that higher-order correlations are an effective way to quantify these subtle structural changes. Higher-order correlation methods can be roughly divided into "order agnostic" methods which assume no *a priori* structures[21–30], and those which more explicitly identify certain geometric motifs, so-called *locally favoured structures* (LFS). These LFS have been identified in a variety of glassforming systems using computer simulation[30–42] and particle-resolved studies in colloid experiments[43–46]. Further evidence of increasing numbers of LFS upon cooling is also found in metallic glassformers[16,47–49].

One of the few studies to examine ageing from a structural perspective is that of Kawasaki and Tanaka[11]. In a nearly hard sphere system, the authors identified a growing structural lengthscale which was long by comparison to some other structural lengthscales[16,50]. This lengthscale had the same relationship with relaxation time in the equilibrium supercooled liquid and ageing glassy systems. Somewhat similar conclusions were reached by Schoenholz *et al.*[51] who concluded that Ageing was governed by their order-agnostic "softness" order parameter.

Ageing may be interpreted from an entropic perspective. The formation of supercooled liquids and glasses is dependent on a fast quench to below the melting temperature, T_m, such that crystallisation is avoided. This typically produces states which are out of equilibrium, with significantly larger entropy than equilibrated states of similar temperature. These states traverse their energy landscape when allowed to age at constant temperature[2], moving through configurations with increasingly low energy until they reach equilibrium. We consider any metastabilities (unstable states which may persist for un-

[a)] Corresponding author: chcpr@bristol.ac.uk

bounded timescales) which may exist as local minima on this energy landscape and describe the evolution of glassy states as travelling between such points[52]. This may be interpreted as a gradual decrease in entropy over time. Importantly, in glassy systems the timescale over which equilibrium would be reached is much longer than that possible in typical experiments[53]. Typically one expects this passage through the energy landscape to slow as the temperature is reduced[54].

The expectation of such temperature-dependent ageing underlies complex phenomena such as the Kovacs effect, where states of different thermal histories can be contrived to have a similar position on the energy landscape[55], which can also be realised with colloidal systems[56]. If we assume that at lower temperatures the glass takes a slower passage through the energy landscape, ageing should slow down at lower temperatures and at sufficiently low temperatures, ageing may be stopped for all practical purposes. Upon bringing the system back to a higher temperature (but still one at which equilibration is not possible on the accessible timescale), it is as if the system is younger than one maintained at the fixed, higher temperature. Such a *transient deep quench* protocol is illustrated in Fig. 1 and has been demonstrated in spin glasses[53]. In this work, we investigate this phenomenon in two atomistic glassformers. Note that this phenomenon, which we shall refer to as a transient deep quench, has been referred to as "rejuvenation"[53], but is distinct from the phenomenon of the same name introduced by Kovacs[55].

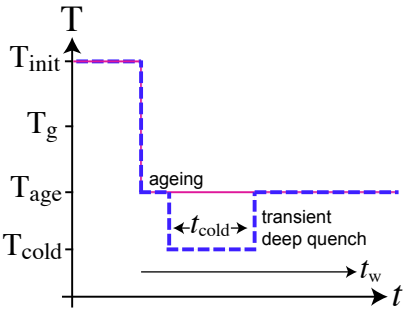

FIG. 1. Schematic showing ageing and rejuvenation protocols used. Ageing (red line) maintains the system at a temperature $T_{\rm age}$ which is between the operational glass transition temperature T_g and T_0. In the case of rejuvenation (dashed blue line), the system spends a period $t_{\rm cold}$ at a lower temperature $T_{\rm cold}$ which may be equal to or less than T_0.

This paper aims to focus on the ageing behaviour of the local structure of the Kob-Andersen[57] and Wahnström[58] binary Lennard-Jones mixtures. We consider the ageing of structural quantities, in particular the potential energy and the population of locally favoured structures, known for each system[39,59]. Remarkably, we find that at the levels of equilibration our simulations access, the rate of ageing of these quantities is independent of ageing temperature, except at temperatures quite close to zero, well below the Vogel-Fulcher-Tamman (VFT) temperature. At this VFT temperature, divergence of the relaxation time may be predicted upon extrapolation[2,60]. Our paper is organised as follows. In our methods section we give a description of our simulation methodology (section II A), dynamical characterisation (section II B), local structural analysis (section II C) and quenching and ageing protocols (section II D). Our results section beings by recapping the equilibrium behaviour (section III A), followed by results for our ageing systems in section III B. We then consider the effect of a transient deep quench upon ageing in section III C. Finally we conclude our findings in section IV.

II. METHODS

A. Simulation Details

Molecular dynamics simulations were conducted with the LAMMPS simulation software[61]. We consider two binary Lennard-Jones mixtures, Kob-Andersen[57] and Wahnström[58]. All simulations were conducted in the NVT ensemble with the temperature regulated using the Nosé-Hoover thermostat algorithm[62], a simulation timestep $\delta t = 0.001$ and number of particles $N = 10648$. Physical quantities are expressed in reduced units, lengths in units of the A species $\sigma_{\rm A}$, energies in units of the well depth for the A species $\varepsilon_{\rm A}$, time in units of $\sqrt{m\sigma_{\rm A}^2/\varepsilon_{\rm A}}$, masses in units of $m_{\rm A}$ and temperatures in units of $k_{\rm B}/\varepsilon_{\rm A}$.

The Kob-Andersen mixture is comprised of A and B type particles of equal mass in a $4:1$ ratio[63]. The number density, $\rho = 1.2$. All parameters are scaled with respect to the A-A interaction: $\varepsilon_{\rm AB} = 1.5\varepsilon_{\rm AA}$, $\varepsilon_{\rm BB} = 0.5\varepsilon_{\rm AA}$, $\sigma_{\rm AB} = 0.80\sigma_{\rm AA}$, $\sigma_{\rm BB} = 0.88\sigma_{\rm AA}$. We take the interaction truncation radius, r_{tr}, as proportional to the interaction lengths between species i.e. $r_{tr}^{\rm AA} = 2.5$, $r_{tr}^{\rm AB} = 2.0$ and $r_{tr}^{\rm BB} = 2.2$[57]. Here we use the temperature at which the dynamics are predicted to diverge by the Vogel-Fulcher-Tamman (VFT) equation [Eq. 3], T_0 to characterise the dynamics. This VFT temperature, $T_0 \approx 0.3$ has been previously reported[59,64–66]. Here we take $T_0 = 0.278$[66].

The Wahnström mixture is comprised of equal numbers of type A and B type particles with masses $m_{\rm B} = 0.5\ m_{\rm A}$. The number density, $\rho = 1.296$. All interaction parameters are scaled with respect to the A-A interaction: $\varepsilon_{\rm AA} = \varepsilon_{\rm AB} = \varepsilon_{\rm BB}$, $\sigma_{\rm AB}/\sigma_{\rm AA} = 11/12$, $\sigma_{\rm BB}/\sigma_{\rm AA} = 5/6$ and all interactions are truncated at a separation of 2.5[58]. A value for the VFT temperature, $T_0 = 0.456$ has been previously reported[39].

B. Dynamical Behaviour

We determine the structural relaxation time, τ_α, from the self-intermediate scattering function (ISF)

$$F(\mathbf{k},t) = \langle \exp[i\mathbf{k}\cdot(\mathbf{x_j}(t) - \mathbf{x_j}(0))]\rangle\,, \tag{1}$$

where $\mathbf{k}$ describes a wavevector in reciprocal space, t represents time and $\mathbf{x_j}(t)$ describes the position of atom j at time t. We determine the structural relaxation time by fitting to a Kolrausch-Williams-Watts (KWW) law

$$F(\mathbf{k},t) = c\exp(-(t/\tau_\alpha)^b), \tag{2}$$

where τ_α is the relaxation time, c is the non ergodicity parameter which describes the height of the plateau before alpha relaxation begins and b is the degree of exponential stretch.

C. Local Structure

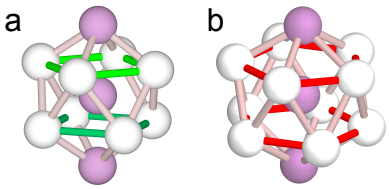

FIG. 2. The locally favoured structures of the systems considered. (a) The bicapped square antiprism found in the Kob-Andersen model. (b) The icosahedron of the Wahnström model.

To identify local structure we use the topological cluster classification (TCC) algorithm[67]. This TCC works by identifying a neighbour network between particles using a Voronoi tessellation and from this, minimum distance rings of 3, 4 and 5 particles are determined. From these structures, larger structures are assembled hierarchically. The TCC analysis has previously been applied to the Kob-Andersen[59,68] and Wahnström[39,68] models. We define the LFS of the system as the geometric motif which minimises the free energy per particle for a small number of particles. For the Wahnström mixture the LFS is the icosahedron while for the Kob-Andersen mixture the LFS is the bicapped square antiprism. These LFS are illustrated in Figure 2. In this work we consider only these two structures; their population is expressed as the number of particles occupying the LFS as a fraction of the number of particles in the system $\langle N_{\mathrm{LFS}}\rangle$.

We have elected to work with instantaneous, thermalised configurations. It would also be possible to carry out our analysis, not on such thermalised configurations, but instead on inherent states obtained from energy minimisation. However, we have found that performing such minimisations leads to a upwards shift in the LFS population by around 0.2 at all temperatures at which we can equilibrate the system. Thus, even at high temperatures (where we do not expect any LFS), analysing inherent states nevertheless yields very considerable numbers of LFS. We conclude that for our purposes, thermalised configurations give a clearer signal.

D. Quenching and Ageing Protocol

We define equilibrium behaviour by monitoring the potential energy per particle. Upon reaching a constant value with time, the system is taken to be in equilibrium, a condition which was consistently fulfilled after a time of $30\tau_\alpha$. When allowed to equilibrate over this timescale, maximum deviations of the potential energy per particle from the mean never exceeded 0.3%. Initial configurations were prepared by quenching the system from $T = 2.0$ to a lower temperature, $T_{\mathrm{init}} = 0.65$, over one timestep (10^{-3} time units). This leads to an instantaneous re-assignment of particle velocities (drawn from a Maxwell-Boltzmann distribution). The Nose-Hoover thermostat then maintains a constant temperature with a damping time $t_{\mathrm{damp}} = 0.1$ in reduced units (100 time steps). For all simulation runs the potential energy and local structure were monitored after quenching for signs of crystallisation which was not observed in any of the simulation runs. Thereafter, the system was allowed to reach equilibrium by simulating in the NVT regime for $30\tau_\alpha$.

To generate unique initial configurations for repeat simulations, the equilibrated sample was evolved successively in the NVT ensemble for a minimum of $10\tau_\alpha$. At this point, the samples were assumed to be decorrelated from one another. To generate non-equilibrium glassy states, these initial samples were quenched in the manner described above to a lower aging temperature T_{age}. These states were evolved at T_{age} with physical properties of the system measured after different waiting times, t_w.

In the case of the transient deep quench protocol, starting from decorrelated supercooled liquid states at T_{init}, the samples were quenched to an operational temperature, T_{age}. They were then allowed to evolve for a period of time. After this, the temperature of the samples was decreased again from, T_{age}, to a lower temperature, T_{cold}. Two values of T_{cold} were evaluated, the VFT temperature, T_0 of the system and $T_{\mathrm{cold}} = 0.1$. The samples were kept at T_{cold} for one decade of time, i.e. from 10^i to 10^{i+1} time units before they were rapidly heated to the operational temperature T_{age}. This protocol was followed for both systems varying both the operational temperature and the time spent initially prior to the first quench to T_{cold}. Our quenching, ageing and rejuvenation protocols are illustrated schematically in Fig. 1.

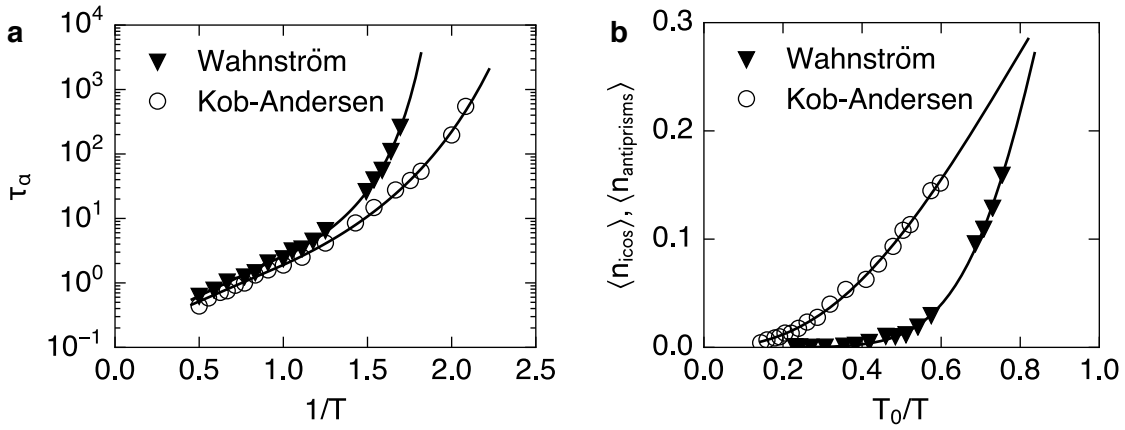

FIG. 3. (a) Angell plot: relaxation time, τ_α, is plotted on a log scale against $1/T$. The VFT law (Eq. 3) is used to fit data in the super Arrhenius region. (b) LFS populations plotted against T_0/T. The LFS of the Wahnström mixture is the icosahedron and the LFS of the Kob-Andersen mixture is the bicapped square antiprism.

III. RESULTS

A. Equilibrium Behaviour

In this section we consider the properties of the studied Lennard-Jones glassformers in meta-equilibrium (metastable to crystallisation). Figure 3(a) shows the Angell plot of $\log \tau_\alpha$ against $1/T$ for both systems. For temperatures below the onset temperature, $T_{\rm on} \approx 1$, the usual super-Arrhenius behaviour of a fragile glassformer is observed. We fit this data with the Vogel-Fulcher-Tammann expression

$$\tau_\alpha = \tau_0 \exp\left(\frac{D}{T - T_0}\right), \tag{3}$$

where the parameter D represents the fragility and $T_0 \approx T_{\rm K}$, the Kauzmann temperature[60]. For T $< T_{\rm on}$, the VFT expression fits the super-Arrhenius data well, yielding parameters in close agreement with previous measurements[39,59]. As previously observed,[34], we see that the Wahnström model is considerably more fragile. For the Wahnström system, $T_0 = 0.460 \pm 0.009$ and for the Kob-Andersen system, $T_0 = 0.287 \pm 0.009$.

Figure 3(b) shows $\langle N_{\rm LFS}\rangle$, determined using the TCC algorithm, as a function of temperature for the two systems. Similarly to τ_α, $\langle N_{\rm LFS}\rangle$ is seen to increase as the temperature of the system decreases. This relationship has been parameterised by Turci *et. al.*[69] in the form:

$$\langle n_{\rm LFS}\rangle = \frac{1}{1 + (T/T_{1/2})^\gamma} \tag{4}$$

This sigmoidal fit describes the growth of from $\langle N_{\rm LFS}\rangle$ 0 at high temperatures to 1 at high temperatures. The fitted parameters are $T_{1/2} = 0.24, 0.47$ and $\gamma = 2.5, 6.6$ for the Kob-Andersen and Wahnström models respectively. The Kob-Andersen model results agree with previously work[69] while the Wahnström model has not been previously parameterised in this way.

In addition to structure and dynamics, we consider the behaviour of the potential energy per atom. As predicted in theory[70] and verified for the Kob-Andersen mixture[64], the potential energy per atom is dominated by a $T^{3/5}$ term:

$$\langle u\rangle = u_0 + AT^{3/5}. \tag{5}$$

We obtain equilibrated samples, whose potential energy per particle is represented in Fig. 4. Fits following Eq. 6 are shown for both models in Fig. 4, giving $A = 2.6, 2.7, u_0 = -9.21, -8.62$ for the Kob-Andersen and Wahnström models respectively.

B. Ageing

Figures 5(a) and (b) show, for the Wahnström and the Kob-Andersen models respectively, the relaxation time τ_α as a function of the waiting time t_w. The structural relaxation time is estimated during ageing by fitting the self-intermediate scattering function (ISF) between time t_w and time t. After a relatively slow growth (sub-ageing) at short times, we find behaviour consistent with power-law growth, $\tau_\alpha \sim t_w^c$, with $c \gtrsim 0.5$. This matches previous results when the waiting time is comparable to the relaxation time[10].

Figure 6 shows plots of potential energy per atom against waiting time, t_w. The initial decay of the energy over short timescales corresponds to the β relaxation process. Following this we see a logarithmic relationship of the form:

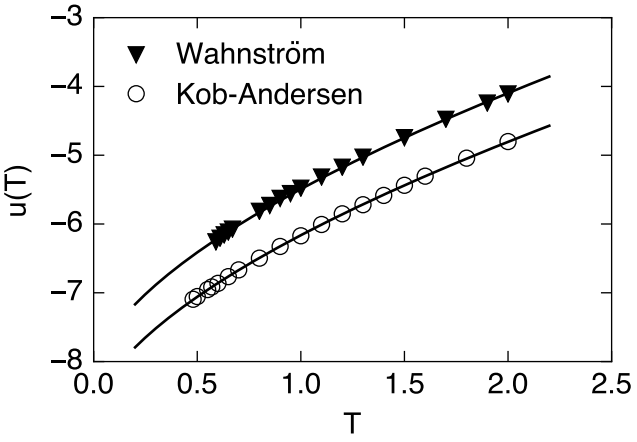

FIG. 4. Potential energy per particle plotted against temperature for the Kob-Andersen and Wahnström systems.

$$u(t_w;T) = m(T)\log(t_w) + C(T). \quad (6)$$

We treat m and C as fitting parameters and note that $m(T)$ is approximately constant, except at the very lowest temperatures, $T \lesssim 0.2$. Thus for much of the temperature regime, our results show that the rate of ageing behaviour, denoted by the gradient of the fitted lines, m, appears to show no temperature dependence. This is contrary our expectation from work on atomic and molecular systems that the ageing dynamics should slow at temperatures around $T_{\rm VFT}$ as found in experiments on molecular systems[12–15].

Figure 7 shows plots of LFS populations for the Kob-Andersen (a) and Wahnström (b) systems respectively. Like the potential energy, the LFS population follows a logarithmic relation at longer waiting times, t_w. This provides evidence that the two quantities, energy and LFS population are closely related. Additionally, comparison between these parameters at short waiting times reinforces this statement: there are two clear changes in gradient of $\langle N_{\rm LFS}\rangle$ at waiting times of approximately 10^{-2} and 10^{0}. We interpret these as corresponding to the two sharp drops in energy visible in Fig. 6 which occur on the timescale of β relaxation $\lesssim 10^{-1}$.

C. Transient Deep Quench

As described in section II D we expected that upon reducing the temperature to $T_{\rm cold}$ following the protocol outlined in Fig. 1, the ageing of the material would be slowed considerably. On the basis of the results presented in section III B by the physical properties of the system, in principle we would then be able to assess what age a sample would have been, had it not been subjected to a period of time at low temperature. However, in section III B we have also seen that ageing in both systems seems to be unaffected by the ageing temperature, so it is unclear that the expectation of a reduced rate of ageing upon a transient deep quench to a lower temperature $T_{\rm cold}$ will be realised.

For both systems we let the system age at temperature $T_{\rm age}$ until $t_w = 10^4$ and then cool the system to the VFT temperature ($T_{\rm cold} = T_0$) and run the system until $t_w = 10^5$. Our reason to select the VFT temperature (rather than, say the same temperature for each system) is to try to make a fair comparison. Since the two models have rather different dynamics at the same temperature, we believe that it is appropriate to take a characteristic temperature and for this reason we select the VFT temperature. We then change the temperature of the thermostat back to the reference ageing temperature $T_{\rm age}$. Under this protocol, therefore, up to $t_w = 10^4$, the procedure is identical to that performed in section III B.

In Fig. 8 we observe that in both systems the potential energy per particle is suddenly reduced when we quench the ageing system to $T_{\rm cold}$. Both systems, however, appear to still slowly age towards lower energy minima. We notice that the Kob-Andersen mixture [Fig. 8(a)] appears to age less than the Wahnström mixture [Fig. 8(b)]. We also notice [inset of Fig.8(a)] that during the transient quench the overall mobility, as measured by the mean squared displacement, is drastically reduced, with the cage size reduced by a factor ~ 0.5.

Figure 9 shows the same behaviour for the population of locally favoured structures $\langle N_{\rm LFS}\rangle$. As the temperature is reduced to $T_{\rm cold}$, a sharp increase in the LFS cluster populations is seen. This is equivalent to forcing the system to lower energy states in the energy landscape and is to be expected. Surprisingly however, these states do not appear to be stable - the system continues to age, forming more LFS clusters. When the system is brought back to the initial ageing temperature $T_{\rm age}$, both the population of locally favoured structures and the energy of the system recover (on logarithmic time scales) their operational values, with no measurable effect from the deep quench in terms of slowing the ageing.

In an attempt to discover if this behaviour was related to the temperature of the deep quench, simulations were performed for the Wahnström mixture at an even colder temperature, $T_{\rm cold} = 0.1$. Our reason to select $T_{\rm cold} = 0.1$ for both systems is that we regard this temperature as rather low, and far below any other relevant temperature for the system (such as the VFT temperature $T_{\rm VFT}$. Indeed we see that, at such low temperatures (Figs. 6 and 7), that the rate of ageing is actually reduced at such very low temperatures. Figure 10 (a) shows the evolution of energy and (b) the LFS population for a deep quench at $T_{\rm cold} = 0.1$. Comparing with Figs. 8 and 9, during the deeply quenched period at $T_{\rm cold}$, we see a reduced rate of ageing in the energy and LFS populations. At the level of our analysis, the observables remain stationary and so we can say ageing appears to cease. However, when these systems are returned to the original ageing tem-

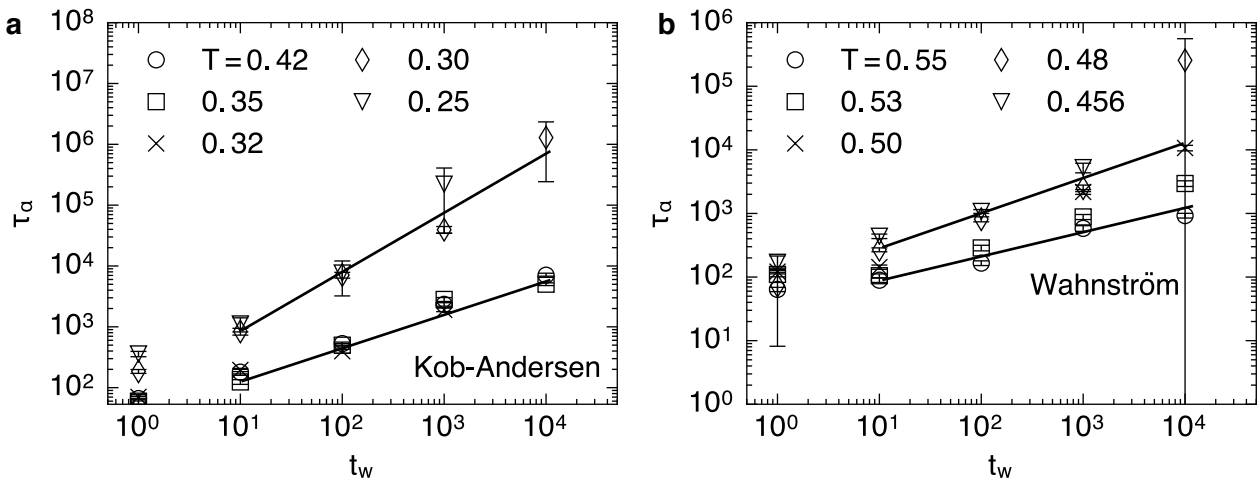

FIG. 5. Relaxation time, τ_α plotted as a function of waiting time t_w for the Kob-Andersen and Wahnström systems at a variety of temperatures. The slope indicates the power-law like behaviour reached on our simulation timescales, $\tau_\alpha \sim {\tau_w}^c$ where $c \gtrsim 0.5$. For the coldest temperatures and longest waiting times, full relaxation is unachievable, hence the large errorbars.

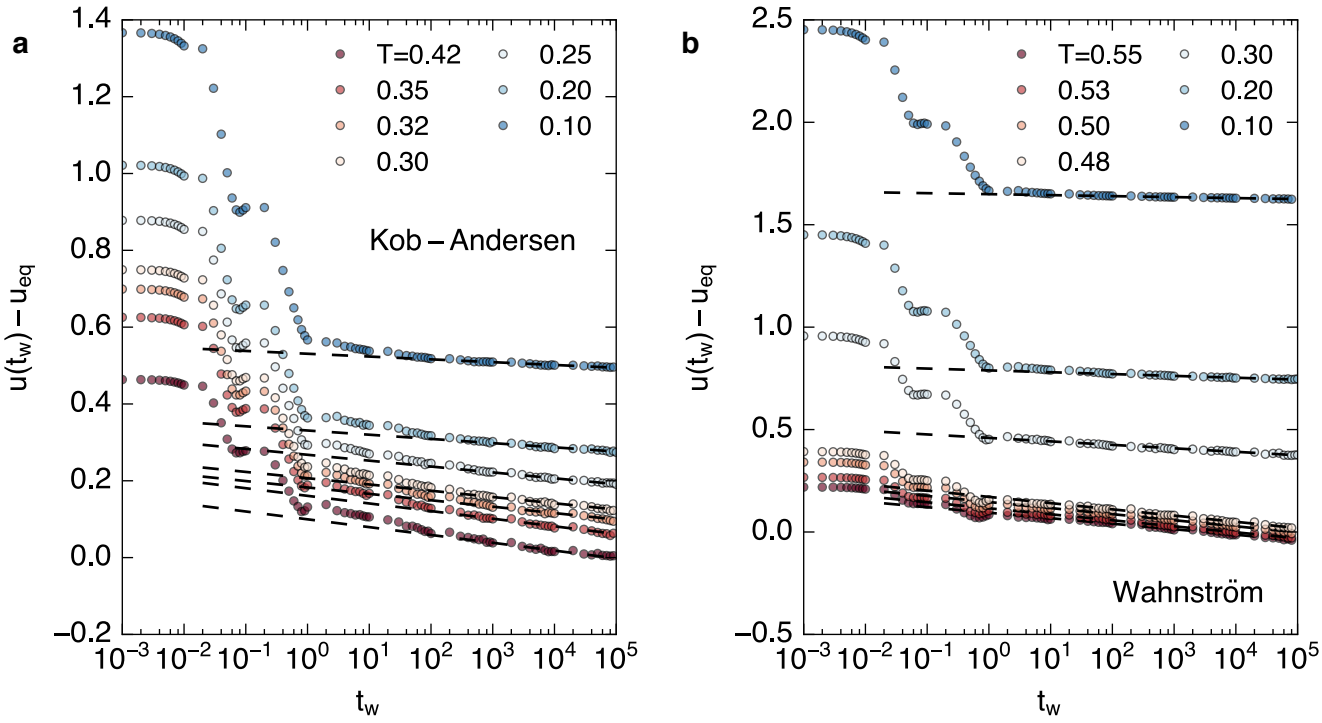

FIG. 6. Potential energy per atom plotted against waiting time, t_w. We plot the difference with respect to the equilibrium value $E_{\rm eq}$ predicted by Eq.6 (valid in principle for $T > T_0$). A logarithmic relationship is observed and has been fitted to the second part of the data. We fit Eq.6 with $m(T)$ in the [-0.030, -0.005], and [-0.020, -0.007] ranges for the Wahnström and the Kob-Andersen models respectively. The initial energy decay is caused by β relaxation effects.

perature, the observables appear to fall on *the same line* extrapolated from before the deep quench. Even though the effects of ageing are not apparent at a quench to $T_{\rm cold} = 0.1$, it appears that the system is able to progress through the energy landscape at the same rate as it does at $T_{\rm age}$.

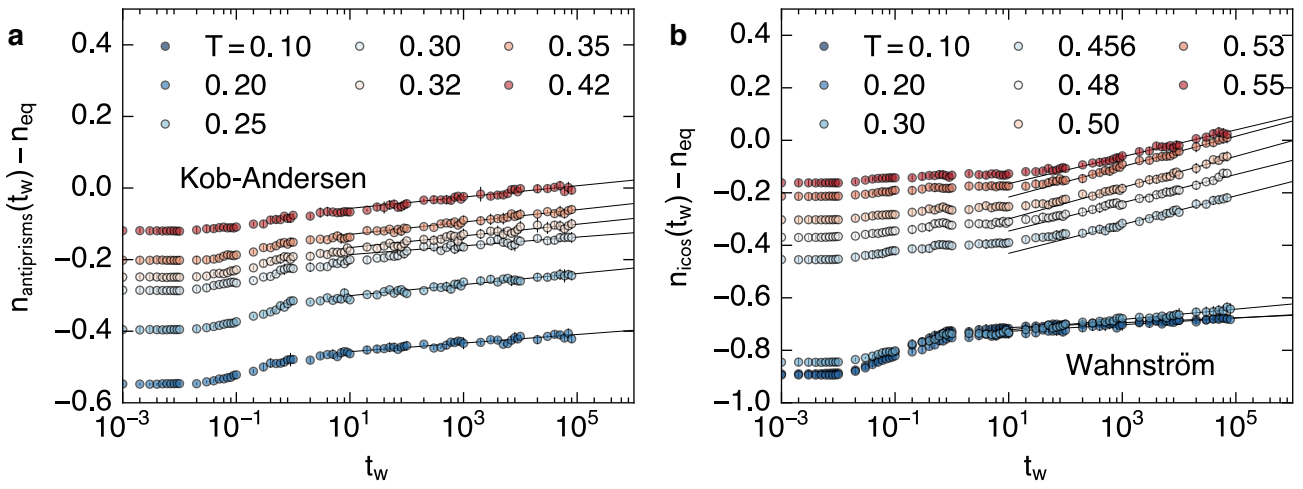

FIG. 7. Locally favoured structure population plotted against waiting time, t_w. A logarithmic relationship is observed and has been fitted at long waiting times. Note that here we subtract the expected equilibrium value of the energy, based on Eq. 4.

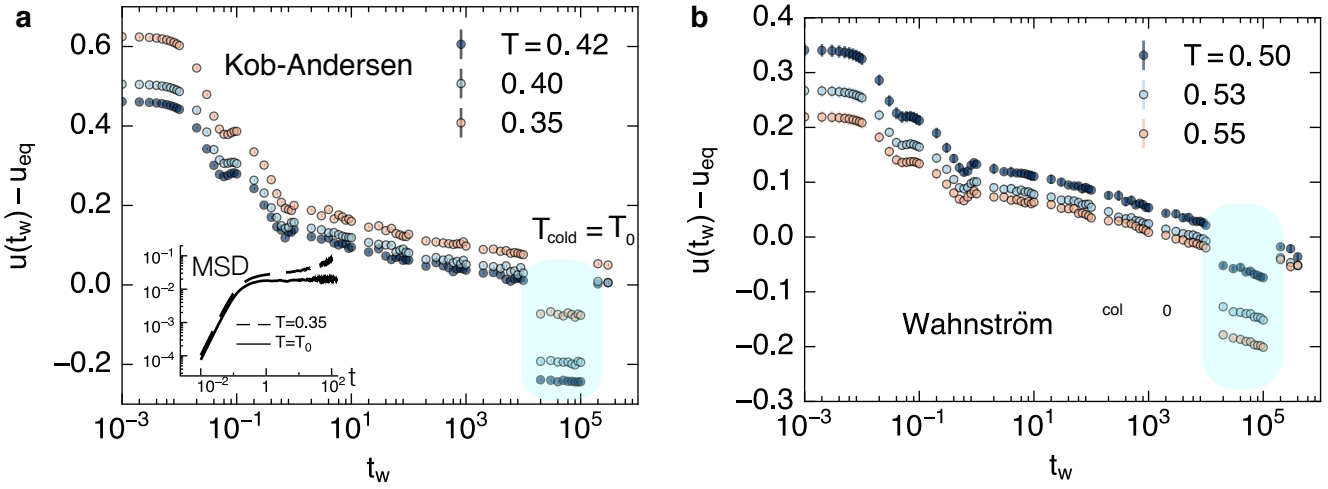

FIG. 8. Evolution of the potential energy per particle during the transient deep quench protocol for the Kob-Andersen (a) and Wahnström (b) model with $T_{\rm cold} = T_0$. Note that we subtract the expected equilibrium value of the energy, based on Eq. 6. Shaded areas denote periods for which the temperature is reduced to $T_{\rm cold}$. Inset of (a): mean squared displacement during ageing at $T = 0.35$ or during the transient deep quench at $T = T_0$.

IV. DISCUSSION AND CONCLUSIONS

The dynamical, structural, and energy behaviour of two binary Lennard-Jones glassformers have been investigated in equilibrium, the "ageing" regime and for a transient deep quench protocol. In equilibrium, structural measurements demonstrated that for both models $\langle N_{\rm LFS}\rangle$ follows a sigmoidal law while the potential energy per particle is dominated by a $T^{3/5}$ term. In the ageing regime, the waiting time dependence of both the energy and the locally favoured structure population were found to follow a logarithmic relationship with the rate unaffected by temperature except for low temperatures, less than around 30% of the Vogel-Fulcher-Tamman temperature. This behaviour is consistent with the work of Gujrati[17]. In the deep quench protocol, we considered the effect of reducing temperature during ageing in order to further slow the motion of the particles. Contrary to our expectation that the system explores the energy landscape at a reduced rate upon quenching, we instead find that the rate of ageing appears unaffected at the temperatures we consider and for the time scales accessible to our numerical simulations. Upon reheating to their original temperatures, energy and LFS population values would reliably overlap their expected trajectories, had they simply been kept at constant temperature.

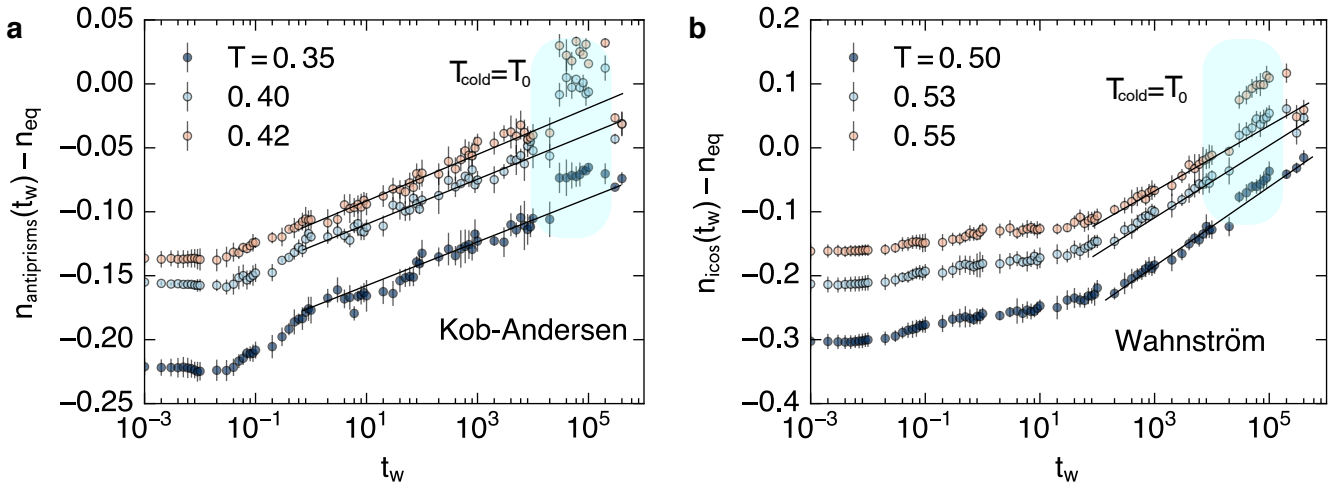

FIG. 9. (a) Evolution of the concentration of LFS during the transient deep quench protocol for the Kob-Andersen and (b) Wahnström model. Ee subtract the expected equilibrium value of the LFS population, based on Eq. 4. Shaded areas denote periods for which the temperature is reduced to $T_{\rm cold}$.

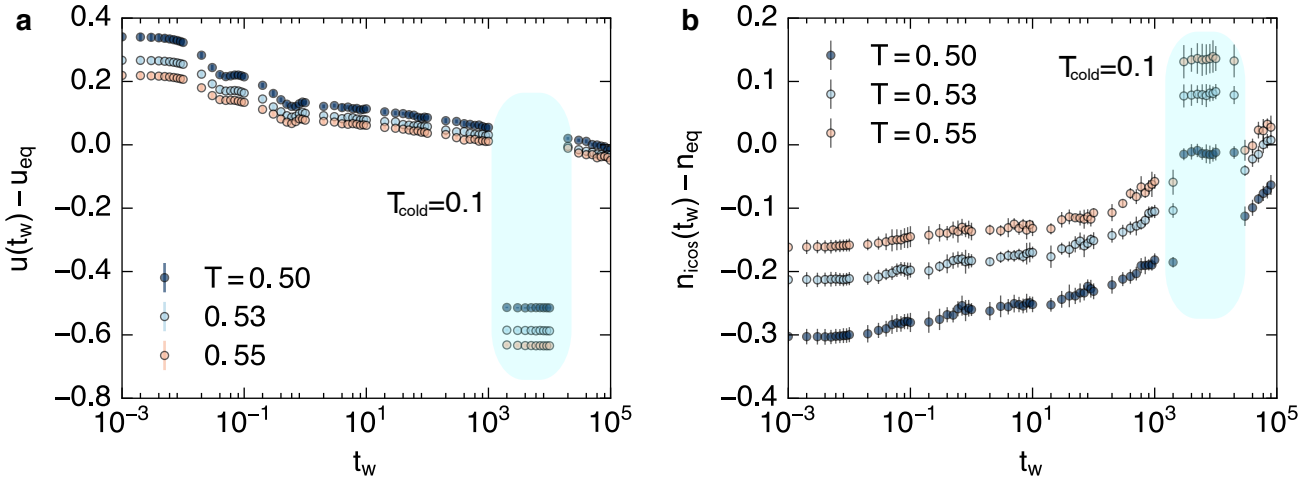

FIG. 10. (a) Evolution of the potential energy per particle and (b) LFS concentration during the transient deep quench protocol for the Wahnström $T_{\rm cold} = 0.1$. We subtract the expected equilibrium value of the energy and LFS populations, based on Eq. 6 and Eq. 4 respectively. Shaded areas denote periods for which the temperature is reduced to $T_{\rm cold}$.

We now address why temperature seems to influence the ageing dynamics so little. Firstly, we note that, clearly, at absolute zero the rate of ageing must drop to zero. At finite temperature, but still very much more deeply supercooled than we can access, in molecular systems it is understood that ageing is slowed at lower temperatures around $T_{\rm VFT}$[12–15]. One very clear difference between these molecular systems and our simulations is the timescale. Here, we have considered a time window of five decades which is considerable by the standards of computer simulation. On the other hand, experiments routinely cover 14 decades and it is quite possible that our simulation models are simply nothing like as deep in the energy landscape initially as the experimental systems. To this end, it would be interesting to study systems much deeper in the energy landscape than we have been able to do. However, while techniques exist to prepare such states in simulation[65,71], the ageing dynamics associated with them seem to lie outside the range of current capabilities. It is possible that particle resolved studies of colloids could be employed to tackle this question[43], alternatively, it may be possible to investigate ageing of molecular systems at higher temperature than the glass transition T_g where they can be equilibrated. Indeed it is possible that there exists some crossover temperature where the aging behaviour familiar from experiments on molecular systems, of a reduced rate of ageing with reduced temperature is recovered, instead of the behaviour

we have found here. Furthermore, our findings might be investigated in other systems, such as model strong glassformers[72]. Intriguingly, in their numerical investigation of hard spheres, Kawasaki and Tanaka appear to find similar behaviour, in the form of a rate of increase of a structural lengthscale which is independent of volume fraction[11].

Furthermore, colloidal systems have recently been shown to exhibit the Kovacs effect, which implies a rate of ageing which depends in the degree of supercooling at which the ageing is carried out[56]. This is intriguing , as colloidal systems access the same kind of timescales accessible to computer simulations here. Therefore it would be interesting in the future to carry out a Kovacs-type investigation with the systems and timescales used here.

In short, while more systems should be investigated, it would seem that the effect we have found may be found in a variety of materials, at the degrees of supercooling accessible to computer simulation. It may be worth exploring its connection with the behaviour of the more deeply supercooled systems found in molecular and atomic experiments.

ACKNOWLEDGMENTS

The authors would like to acknowledge Eric Vincent for introducing them to rejuvenation. This work was carried out using the computational facilities of the Advanced Computing Research Centre, University of Bristol. The open source molecular dynamics package LAMMPS[61] was used for molecular dynamics simulations. CPR acknowledges the Royal Society and Kyoto University SPIRITS fund. PC, FT and CPR thank the European Research Council (ERC Consolidator Grant NANOPRS, project number 617266) for financial support

[1] P. Anderson, "Through the glass lightly," Science **267**, 1609–1618 (1995).
[2] L. Berthier and G. Biroli, "Theoretical perspective on the glass transition and amorphous materials," Rev. Mod. Phys. **83**, 587–645 (2011).
[3] M. D. Ediger and P. Harrowell, "Perspective: Supercooled liquids and glasses," J. Chem. Phys. **137**, 080901 (2012).
[4] W. Kob and J. L. Barrat, "Aging effects in a lennard-jones glass," Phys. Rev. Lett. **78**, 4581–4584 (1997).
[5] R. E. Courtland and E. R. Weeks, "Direct visualization of ageing in colloidal glasses," J. Phys.: Condens. Matter **15**, S359–S365 (2003).
[6] D. El Masri, M. Pierno, L. Berthier, and L. Cipelletti, "Ageing and ultra-slow equilibration in concentrated colloidal hard spheres," J. Phys.: Condens. Matter **17**, S3543 (2005).
[7] V. A. Martinez, G. Bryant, and W. Van Megen, "Slow dynamics and aging of a colloidal hard sphere glass," Phys. Rev. Lett **101**, 135702 (2008).
[8] M. Warren and J. Rottler, "Atomistic mechanism of physical ageing in glassy materials," EuroPhys. Lett. **88**, 58005 (2009).
[9] D. El Masri, L. Berthier, and L. Cipelletti, "Subdiffusion and intermittent dynamic fluctuations in the aging regime of concentrated hard spheres," Phys. Rev. E **82**, 031503 (2010).
[10] M. Warren and J. Rottler, "Quench, equilibration, and subaging in structural glasses," Phys. Rev. Lett. **110**, 025501 (2013).
[11] T. Kawasaki and T. H., "Structural evolution in the aging process of supercooled colloidal liquids," Phys. Rev. E **89**, 062315 (2014).
[12] T. Hecksher, N. B. Olsen, K. Niss, and J. C. Dyre, "Physical aging of molecular glasses studied by a device allowing for rapid thermal equilibration," J. Chem. Phys. **133**, 174514 (2010).
[13] B. Ruta, Y. Chushkin, G. Monaco, L. Cipelletti, E. Pineda, P. Bruna, V. M. Giordano, and M. Gonzalez-Silveira, "Atomic-scale relaxation dynamics and aging in a metallic glass probed by x-ray photon correlation spectroscopy," Phys. Rev. Lett. (2012).
[14] Y. P. Koh and S. L. Simon, "Enthalpy recovery of polystyrene: Does a long-term aging plateau exist?" Macromolecules **46**, 5815–5821 (2013).
[15] J. Zhao, S. L. Simon, and G. B. McKenna, "Using 20-million-year-old amber to test the super-arrhenius behaviour of glass-forming systems," Nature Comm. **4**, 1783 (2013).
[16] C. P. Royall and S. R. Williams, "The role of local structure in dynamical arrest," Phys. Rep. **560**, 1 (2015).
[17] P. Gujrati, "Nonequilibrium thermodynamics: Structural relaxation, fictive temperature, and tool-narayanaswamy phenomenology in glasses," Phys. Rev. E **81**, 051130 (2010).
[18] A. Q. Tool, "Relation between inelastic deformability and thermal expansion of glass in its annealing range," J. Am. Ceram. Soc. **29**, 240–253 (1946).
[19] O. S. Narayanaswamy, J. Am. Ceram. Soc. **54**, 491 (1971).
[20] R. L. Leheny, M. Narayanan, S. R. Nagel, D. L. Price, K. Suzuya, and P. Thiyagarajan, "Structural studies of an organic liquid through the glass transition," J. Chem. Phys. **105**, 7783–7794 (1996).
[21] J. Kurchan and D. Levin, "Order in glassy systems," ArXiV:cond-mat **1008.4068v1** (2009).
[22] F. Sausset and D. Levine, "Characterizing order in amorphous systems," Phys. Rev. Lett. **107**, 045501 (2011).
[23] C. Cammarota and G. Biroli, "Ideal glass transitions by random pinning." Proc. Nat. Acad. Sci **109**, 8850–5 (2012).
[24] C. Cammarota and G. Biroli, "Patch-repetition correlation length in glassy systems," EuroPhys. Lett. **98**, 36005 (2012).
[25] A. J. Dunleavy, K. Wiesner, and C. P. Royall, "Using mutual information to measure order in model glass-formers," Phys. Rev. E **86**, 041505 (2012).
[26] E. D. Cubuk, S. S. Schoenholz, J. M. Rieser, B. D. Malone, J. Rottler, D. J. Durian, E. Kaxiras, and A. J. Liu, "Identifying structural flow defects in disordered solids using machine-learning methods," Phys. Rev. Lett. **114**, 108001 (2015).
[27] S. Albert, T. Bauer, M. Michl, G. Biroli, J.-P. Bouchaud, A. Loidl, P. Lunkenheimer, R. Tourbot, C. Wiertel-Gasquet, and F. Ladieu, "Fifth-order susceptibility unveils growth of thermodynamic amorphous order in glass-formers," Science **352**, 1308–1311 (2016).
[28] S. S. Schoenholz, E. D. Cubuk, D. M. Sussman, E. Kaxiras, and A. J. Liu, "A structural approach to relaxation in glassy liquids," **12**, 469–471 (2016).
[29] P. Charbonneau, E. Dyer, J. Lee, and S. Yaida, "Linking dynamical heterogeneity to static amorphous order," J. Stat. Mech.: Theory and Experiment , 074004 (2016).
[30] D. Coslovich and R. L. Jack, "Structure of inactive states of a binary lennard-jones mixture," J. Stat. Mech.: Theory and Experiment , 074012 (2016).
[31] P. J. Steinhardt, D. R. Nelson, and M. Ronchetti, "Bond-orientational order in liquids and glasses," Phys. Rev. B **28**, 784–805 (1983).
[32] H. Jonsson and H. C. Andersen, "Icosahedral ordering in the lennard-jones liquid and glass," Phys. Rev. Lett. **60**, 2295–2298 (1988).
[33] M. Dzugutov, S. I. Simdyankin, and F. H. M. Zetterling, "Decoupling of diffusion from structural relaxation and spatial heterogeneity in a supercooled simple liquid," Phys. Rev. Lett. **89**, 195701 (2002).
[34] D. Coslovich and G. Pastore, "Understanding fragility in supercooled lennard-jones mixtures. i. locally preferred structures," J. Chem. Phys **127**, 124504 (2007).

[35] J.-P. Eckmann and I. Procaccia, "Ergodicity and slowing down in glass-forming systems with soft potentials: No finite-temperature singularities," Phys. Rev. E **78**, 011503 (2008).

[36] E. Lerner, I. Procaccia, and J. Zylberg, "Statistical Mechanics and Dynamics of a Three-Dimensional Glass-Forming System," Phys. Rev. Lett. **102**, 125701 (2009).

[37] F. Sausset and G. Tarjus, "Growing static and dynamic length scales in a glass-forming liquid." Phys. Rev. Lett. **104**, 065701 (2010).

[38] H. Tanaka, T. Kawasaki, H. Shintani, and K. Watanabe, "Critical-like behaviour of glass-forming liquids." Nature materials **9**, 324–31 (2010).

[39] A. Malins, J. Eggers, C. P. Royall, S. R. Williams, and H. Tanaka, "Identification of long-lived clusters and their link to slow dynamics in a model glass former," J. Chem. Phys. **138**, 12A535 (2013).

[40] G. M. Hocky, D. Coslovich, A. Ikeda, and D. Reichman, "Correlation of local order with particle mobility in supercooled liquids is highly system dependent," Phys. Rev. Lett. **113**, 157801 (2014).

[41] C. P. Royall, A. Malins, A. J. Dunleavy, and R. Pinney, "Strong geometric frustration in model glassformers," J. Non-Cryst. Solids **407**, 34–43 (2014).

[42] N. Dougan, P. Crowther, C. P. Royall, and F. Turci, "Controlling local order of athermal self-propelled particles," J. Stat. Mech.: Theory and Experiment , 124001 (2016).

[43] A. Ivlev, H. Loewen, G. E. Morfill, and C. P. Royall, *Complex Plasmas and Colloidal Dispersions: Particle-resolved Studies of Classical Liquids and Solids* (World Scientific Publishing Co., Singapore Scientific, 2012).

[44] C. Royall, S. Williams, T. Ohtsuka, and H. Tanaka, "Direct observation of a local structural mechanism for dynamic arrest," Nature Materials **7**, 556 (2008).

[45] S. Mazoyer, F. Ebert, G. Maret, and P. Keim, "Correlation between dynamical heterogeneities, structure and potential-energy distribution in a 2d amorphous solid," Eur. Phys. J. E **34**, 101 (2011).

[46] M. Leocmach and H. Tanaka, "Roles of icosahedral and crystal-like order in the hard spheres glass transition," Nat. Comm. **3**, 974 (2012).

[47] Y. Q. Cheng and E. Ma, "Atomic-level structure and structure-property relationship in metallic glasses," Prog. Mat. Sci. **56**, 379473 (2011).

[48] A. Hirata, P. Guan, T. Fujita, Y. Hirotsu, A. Inoue, Y. A. R., T. Sakurai, and M. Chen, "Direct observation of local atomic order in a metallic glass," Nature Mater. **10**, 28–33 (2010).

[49] A. C. Y. Liu, M. J. Neish, G. Stokol, G. A. Buckley, L. A. Smillie, M. D. de Jonge, R. T. Ott, M. J. Kramer, and L. Bourgeois, "Systematic mapping of icosahedral short-range order in a melt-spun $zr_{36}cu_{64}$ metallic glass," Phys. Rev. Lett. **110**, 205505 (2013).

[50] S. Karmakar, C. Dasgupta, and S. Sastry, "Growing length scales and their relation to timescales in glass-forming liquids," Annu. Rev. Cond. Matt. Phys. **5**, 255–284 (2014).

[51] S. S. Schoenholz, E. D. Cubuk, E. Kaxiras, and A. J. Liu, "Relationship between local structure and relaxation in out-of-equilibrium glassy systems," Proc. Nat. Acad. Sci. **114**, 263–267 (2017).

[52] M. Goldstein, "Viscous liquids and the glass transition : a potential energy landscape picture," J. Chem. Phys. **51**, 3728–3739 (1969).

[53] E. Vincent, "Ageing, rejuvenation and memory: the example of spin-glasses," in *Ageing and the glass transition* (Springer, 2007) pp. 7–60.

[54] D. J. Wales, *Energy Landscapes: Applications to Clusters, Biomolecules and Glasses* (Cambridge University Press, Cambridge, 2004).

[55] G. McKenna, "Comprehensive polymer science," (Pergamon, Oxford, 1989) Chap. Polymer Properties, p. 311362.

[56] X. Di, K. Z. Win, G. B. McKenna, T. Narita, F. Lequeux, S. Rao Pullela, and Z. Cheng, "Signatures of structural recovery in colloidal glasses," Phys. Rev. Lett. **106**, 095701 (2011).

[57] W. Kob and H. Andersen, "Testing mode-coupling theory for a supercooled binary lennard-jones mixture i: The van hove correlation function," Phys. Rev. E **51**, 4626–4641 (1995).

[58] G. Wahnström, "Molecular-dynamics study of a supercooled two-component lennard-jones system," Phys. Rev. A **44**, 3752–3764 (1991).

[59] A. Malins, J. Eggers, H. Tanaka, and C. P. Royall, "Lifetimes and lengthscales of structural motifs in a model glassformer," Faraday Discussions **167**, 405–423 (2013).

[60] A. Cavagna, "Supercooled liquids for pedestrians," Phys. Rep. **476**, 51–124 (2009).

[61] S. Plimpton, "Fast parallel algorithms for short-range molecular dynamics," J. Comp. Phys. **117**, 1 – 19 (1995).

[62] D. J. Evans and B. L. Holian, "The nose–hoover thermostat," J. Chem. Phys. **83**, 4069–4074 (1985).

[63] W. Kob and H. C. Andersen, "Scaling behavior in the beta-relaxation regime of a supercooled lennard-jones mixture," Phys. Rev. Lett. **73**, 1376–1379 (1994).

[64] F. Sciortino, W. Kob, and P. Tartaglia, "Inherent structure entropy of supercooled liquids," Phys. Rev. Lett. **83**, 3214–3217 (1999).

[65] T. Speck, A. Malins, and C. P. Royall, "First-order phase transition in a model glass former: Coupling of local structure and dynamics," Phys. Rev. Lett. **109**, 195703 (2012).

[66] P. Crowther, F. Turci, and R. C. P., "The nature of geometric frustration in the kob-andersen mixture," J. Chem. Phys. **143**, 044503 (2015).

[67] A. Malins, S. R. Williams, J. Eggers, and C. P. Royall, "Identification of structure in condensed matter with the topological cluster classification," J. Chem. Phys. **139**, 234506 (2013).

[68] C. P. Royall, A. Malins, A. J. Dunleavy, and R. Pinney, "Strong geometric frustration in model glassformers," J. Non-Cryst. Solids **407**, 34–43 (2015).

[69] F. Turci, C. P. Royall, and T. Speck, "Non-equilibrium phase transition in an atomistic glassformer: the connection to thermodynamics," arXiv , 1603.06892 (2016).

[70] Y. Rosenfeld and P. Tarazona, "Density functional theory and the asymptotic high density expansion of the free energy of classical solids and fluids," Mol. Phys **95**, 141—150 (1998).

[71] L. Berthier and R. L. Jack, "Evidence for a disordered critical point in a glass-forming liquid," Phys. Rev. Lett. **114**, 205701 (2015).

[72] D. Coslovich and G. Pastore, "Dynamics and energy landscape in a tetrahedral network glass-former: direct comparison with models of fragile liquids," J. Phys.: Condens. Matter **21**, 285107 (2009).